TA 81

A STEADY–STATE PARTICLE METHOD FOR THE BOLTZMANN EQUATION

JENS STRUCKMEIER*

Abstract. We present a particle method for the numerical simulation of boundary value problems for the steady–state Boltzmann equation. Referring to some recent results concerning steady–state schemes, the current approach may be used for multi–dimensional problems, where the collision scattering kernel is not restricted to Maxwellian molecules. The efficiency of the new approach is demonstrated by some numerical results obtained from simulations for the (two–dimensional) Benard's instability in a rarefied gas flow.

Key words. rarefied gas flows, steady Boltzmann equation, particle methods

AMS subject classifications. 76P05, 82C80, 65C05

1. Introduction. The dynamic behaviour of a rarefied gas is described by the Boltzmann equation, the fundamental transport equation in the kinetic theory of gas flows. The Boltzmann transport equation uses a mesoscopic picture of a rarefied gas: macroscopic quantities, like the mass density or the temperature, are obtained from the moments of the density function described by the Boltzmann equation. On the other hand, the dynamic behaviour of the density itself, as given by the Boltzmann equation, is derived from a microscopic picture, where one considers the molecular dynamic of single particles, in the limit, when the particle number in the gas tends to infinity.

Besides the more theoretical problems concerning the Boltzmann equation, the numerical simulation of rarefied gas flows plays a central role in the kinetic theory of gases. In particular, due to the ongoing speed up of the existing computer hardware, above all massively–parallel systems, one is able to perform complex three–dimensional simulations of rarefied gas flows, even close to the continuum regime, including real gas effects and chemical reactions in a gas mixture.

Numerical simulation techniques are nearly exclusively based on so–called particle methods, where one uses a finite set of particles to approximate the density function described by the Boltzmann equation. Moreover, these particle methods are in general applied to time–dependent problems, i.e. the time–dependent Boltzmann equation, although a lot of applications in the kinetic theory of gases are described by boundary value problems for the steady–state equation.

The derivation of time–dependent particle methods is based on a splitting scheme, which separates the two phenomena appearing in a rarefied gas, namely the free transport of gas particles in the spatial domain and the binary collisions between gas particles. The treatment of collisions uses in general an explicit time difference scheme for the space–homogeneous Boltzmann equation, which leads to a first order scheme in time together with a restriction on the size of the time step. Hence, one may think about to improve the accuracy of the time integration using higher order schemes as well as to obtain more robust schemes using an implicit time integration. Here, time–dependent particle schemes may be called robust, if they include a control on the conserved quantities of the Boltzmann equation (during the simulation of binary collisions).

*Department of Mathematics, University of Kaiserslautern, P.O Box 3049, 67653 Kaiserslautern, Germany (struckm@mathematik.uni-kl.de).

Besides the derivation of generalized integration techniques, which lead to more flexible particle methods for time–dependent problem, there is still a need to obtain a particle method, which can directly applied to the steady–state equation. In Ref. [1], Babovsky discussed time averaging techniques, when applying a time–dependent particle method to stationary kinetic equations. The material presented there clearly indicates, that a time–dependent code yields in general deviations from the steady–state solution, due to some systematic errors.

In the present paper we discuss a particle method for the steady–state Boltzmann equation, which was recently introduced by Bobylev and the author in Refs. [4] and [5]. The idea is to apply an iteration process directly to the steady–state equation, which is derived from a formal solution of the steady–state problem. This approach was restricted to one–dimensional problems with Maxwellian molecules and the aim of the current investigation is to show, how to use a similar method in the case of a multi–dimensional setup and arbitrary scattering kernels.

2. A Steady–State Particle Method. The steady–state Boltzmann equation (for Maxwellian molecules) on a bounded domain $\Omega \subset I\!R^n$, $n \geq 1$ is given by

$$\mathbf{v} \cdot \nabla f + \frac{\rho(\mathbf{x})}{\varepsilon} f = \frac{1}{\varepsilon} Q_+(f) \tag{2.1}$$

together with appropriate boundary conditions on $\partial\Omega$. Here, the collision operator $Q_+(f)$ is given by

$$Q_+(f) = \int_{I\!R^3} \int_{S^2} g\left(\frac{(\mathbf{v}-\mathbf{v}_*, \mathbf{n})}{|\mathbf{v}-\mathbf{v}_*|}\right) f(\mathbf{v}') f(\mathbf{v}'_*) \mathrm{d}\omega(\mathbf{n}) \mathrm{d}\mathbf{v}_*$$

where $\mathbf{v}'$ and $\mathbf{v}'_*$ are the post–collisional velocities, which can be expressed in the center–of–mass system in the form

$$\mathbf{v}' = \frac{1}{2}\left(\mathbf{v} + \mathbf{v}_* - \|\mathbf{v}-\mathbf{v}_*\|\mathbf{n}\right) \quad \mathbf{v}'_* = \frac{1}{2}\left(\mathbf{v} + \mathbf{v}_* + \|\mathbf{v}-\mathbf{v}_*\|\mathbf{n}\right)$$

g is the (normalized) angular–dependent scattering kernel for Maxwellian molecules and $\rho(\mathbf{x})$ denotes the mass density, i.e. $\rho(\mathbf{x}) = \int f(\mathbf{x}, \mathbf{v}) \mathrm{d}\mathbf{v}$.
For one–dimensional problems, i.e. $\Omega = [0, L] \subset I\!R$, one may simplify Eq. (2.1) by introducing the so–called mass coordinate y, which is defined by

$$y = \int_0^x \rho(x') \mathrm{d}x'$$

Then, the one–dimensional steady–state Boltzmann equation reads

$$\varepsilon v_y \frac{\partial f}{\partial y} + f = \frac{1}{\rho(y)} Q_+(f) \tag{2.2}$$

where v_y denotes the velocity along the slab geometry $[0, L]$.
In Ref. [4] it was proposed to solve the one–dimensional steady–state equation directly using an iterative process given by

$$f^{(n+1)}(y, \mathbf{v}) = \langle \mathrm{e}^{-t v_y \frac{\partial}{\partial y}} F(f^{(n)}) \rangle, \tag{2.3}$$

where $F(f) = \frac{1}{\rho}Q_+(f)$ and the bracket denotes the time–averaging

$$\langle \Psi(t) \rangle = \int_0^\infty \mathrm{e}^{-t/\varepsilon} \Psi(t) \frac{\mathrm{d}t}{\varepsilon}$$

REMARK 2.1. This iterative process is derived formally as follows: the steady–state solution of (2.2) may be expressed by

$$f(y, \mathbf{v}) = (1 + \varepsilon D)^{-1} \frac{1}{\rho(y)} Q_+(f)$$

where D denotes the differential operator $v_y \frac{\partial}{\partial y}$. Now the inverse of the operator $(1 + \varepsilon D)$ can be written in the form

$$(1 + \varepsilon D)^{-1} = \int_0^\infty \mathrm{e}^{-t(1+\varepsilon D)} \mathrm{d}t = \frac{1}{\varepsilon} \int_0^\infty \mathrm{e}^{-t/\varepsilon} \mathrm{e}^{-tD} \mathrm{d}t, \tag{2.4}$$

such that the formal solution reads

$$f(y, \mathbf{v}) = \langle \mathrm{e}^{-tD} \frac{1}{\rho} Q_+(f) \rangle \tag{2.5}$$

which yields an implicit equation for $f(y, \mathbf{v})$. The natural way to solve (2.5) is to apply an iteration

$$f^{(n+1)}(y, \mathbf{v}) = \langle \mathrm{e}^{-tD} \frac{1}{\rho} Q_+(f^{(n)}) \rangle$$

and this exactly yields the equation given above.

The crucial point is, that the iterative process is in particular suited when applying a particle method to simulate rarefied gas flows:

1. using the previous results on particle methods for the time–dependent Boltzmann equation, like discussed in the review article [7], it is straightforward how to derive a particle approximation for the expression $\frac{1}{\rho}Q_+(f)$, assuming that an approximation for the density f is given.

2. the operator exponential $\mathrm{e}^{-tD} \overset{o}{f}$ is simply the solution of the free flow equation

$$\frac{\partial f}{\partial t} + v_y \frac{\partial f}{\partial y} = 0$$

together with the initial condition $f(0, y, \mathbf{v}) = f_0(y, \mathbf{v})$. Moreover, one is able to incorporate the corresponding boundary conditions into this free flow equation.

It remains to discuss the meaning of the time averaging $\langle \cdot \rangle$ over the Poisson distribution with mean value ε: suppose that a particle approximation in the form $\{(\alpha_i, y_i, \mathbf{v}_i)\}_{i=1,\ldots,n}$ for the expression $\frac{1}{\rho}Q_+$ is given. Then applying the operator e^{-tD} on $\frac{1}{\rho}Q_+$ means to solve for the given particle ensemble the characteristic system

$$\dot{y}_i = (v_y)_i \quad \dot{\mathbf{v}}_i = 0$$

Now, the time averaging $\langle \cdot \rangle$ may be realized by choosing for each particle an individual Poisson–distributed time step t_i and to solve the characteristic equations on the time interval $[0, t_i]$.

REMARK 2.2. Formally, this method is derived by considering the weak formulation of the iteration (2.3), i.e.

$$\int_0^L \int_{\mathbb{R}^3} \Phi(y,\mathbf{v}) f^{(n+1)}(y,\mathbf{v}) \mathrm{d}\mathbf{v}\mathrm{d}y = \int_0^L \int_{\mathbb{R}^3} \Phi(y,\mathbf{v}) \langle \mathrm{e}^{-tD} \frac{1}{\rho} Q_+(f^{(n)}) \rangle \mathrm{d}\mathbf{v}\mathrm{d}y$$

The corresponding equation in terms of measures reads

$$\mu^{(n+1)} = (\kappa \times \nu^{(n)}) \circ T^{-1}$$

where κ denotes the measure with density $\frac{1}{\varepsilon}\mathrm{e}^{-t/\varepsilon}$ on $\mathbb{R}_+$, T^{-1} denotes the free stream operator

$$T^{-1}(t, f(t,y,\mathbf{v})) = f(y + tv_y, \mathbf{v})$$

and $\mu^{(n+1)}$ is the measure with density $f^{(n+1)}(y,\mathbf{v})$. Moreover, $\nu^{(n)}$ represents the gain term $\frac{1}{\rho}Q_+$ due to collisions of the measure $\mu^{(n)}$ with density $f^{(n)}$ and may be expressed in the usual way by

$$\nu^{(n)} = (\mu^{(n)} \times \mu^{(n)} \times \omega) \circ P^{-1}$$

with

$$P(\mathbf{v}, \mathbf{v}_*, \mathbf{n}) = \frac{1}{2}(\mathbf{v} + \mathbf{v}_* - \|\mathbf{v} - \mathbf{v}_*\|\mathbf{n})$$

REMARK 2.3. If one does not pass to the mass coordinate y, the resulting characteristic system reads

$$\dot{x} = \frac{1}{\rho(x)} v_x \quad \dot{\mathbf{v}} = 0$$

and the solution on the basis of a particle ensemble is no longer trivial. This is the reason, why the result presented in Ref. [5] is restricted to the one–dimensional case.

The resulting particle scheme for the one–dimensional steady–state equation on the basis of the iterative process given above is quite similar to time–dependent schemes and one may interpret the scheme as a generalization of the classical splitting method:

1. in the free flow step, each particle is equipped with an individual time step, which is Poisson–distributed with mean value $\langle t \rangle = \varepsilon$, whereas in a time–dependent scheme, the particles are moved according to the given time step Δt,

2. in the collision step, each particle undergoes a collision, i.e. no collision probability appears in the simulation, whereas in a time–dependent scheme the collision probability is proportional to the time step Δt.

In Ref. [5] this steady–state approach was used to simulate the one–dimensional steady heat transfer problem with diffusive boundary conditions and the numerical results showed, that the steady–state scheme yields a much faster convergence compared to a time–dependent scheme, at least for Knudsen numbers around unity. In the next sections we describe, how the results may be generalized to the multi–dimensional case with arbitrary collision scattering kernels.

2.1. The Multi–Dimensional Equation for Maxwellian Molecules. The natural generalization of the iterative process from the previous section is to write the formal solution of multi–dimensional Boltzmann equation (2.1) as

$$f(\mathbf{x},\mathbf{v}) = (1 + \frac{\varepsilon}{\rho(\mathbf{x})}\mathbf{v}\nabla)^{-1}\frac{1}{\rho(\mathbf{x})}Q_+(f)$$

and to apply the iteration

$$f^{(n+1)}(\mathbf{x},\mathbf{v}) = (1 + \frac{\varepsilon}{\rho^{(n)}(\mathbf{x})}\mathbf{v}\nabla)^{-1}\frac{1}{\rho^{(n)}}Q_+(f^{(n)})$$

Together with the operator identity (2.4), the direct analogon to (2.3) is given by

$$f^{(n+1)}(\mathbf{x},\mathbf{v}) = \langle \mathrm{e}^{-tD^{(n)}}\frac{1}{\rho^{(n)}}Q_+(f^{(n)})\rangle \tag{2.6}$$

where the bracket denotes again a time–averaging over the Poisson–distribution and $D^{(n)} = \mathbf{v}\cdot\nabla/\rho^{(n)}(\mathbf{x})$.
Although this is the natural generalization from the previous section, applying a particle method is more complicated, because the operator $D^{(n)}$ depends on the macroscopic density of the nth iteration step: if we define $g(t,\mathbf{x},\mathbf{v}) = \mathrm{e}^{-tD^{(n)}}\frac{1}{\rho^{(n)}}Q_+(f^{(n)})$, then g is the solution of the free flow equation

$$\frac{\partial g}{\partial t} + \frac{\mathbf{v}}{\rho^{(n)}(\mathbf{x})}\nabla g = 0 \tag{2.7}$$

with initial condition $\frac{1}{\rho^{(n)}}Q_+(f^{(n)})$. Eq. (2.7) is solved by the characteristic system

$$\dot{\mathbf{x}} = \frac{1}{\rho^{(n)}(\mathbf{x})}\mathbf{v} \quad \dot{\mathbf{v}} = 0$$

which yields a nonlinear system.
In particular, applying a particle method to the iterative process (2.6), one has to use a certain smoothing kernel $\beta^{\Delta}(\mathbf{x},\mathbf{x}_*)$ to derive the density $\rho^{(n)}$ at some point $\mathbf{x}\in\Omega$, i.e.

$$\rho^{(n)}(\mathbf{x}) = \int_{\Omega}\beta^{\Delta}(\mathbf{x},\mathbf{x}_*)\mathrm{d}\delta_{\mu^{(n)}(\mathbf{x}_*,\mathbf{v})}$$

where $\delta_{\mu^{(n)}(\mathbf{x}_*,\mathbf{v})}$ denotes a particle approximation of the density $f^{(n)}$. Even using the standard smoothing kernel, which defines a partition of Ω into a fixed cell system, yields a complicated system of differential equations for the particle trajectories. Moreover, due to the fluctuations, which are inherently contained using a particle method, one might expect some deviations or numerical artifacts using this kind of approach.
Hence, the generalization of the one–dimensional method to obtain a steady–state scheme, where one overcomes the problem by introducing the mass coordinate, to the multi–dimensional case is not trivial.

In the following we describe a new approach, which leads to a characteristic system like in the one–dimensional case. To perform the analysis, we have to assume, that the densities $\rho^{(n)}(\mathbf{x})$ are bounded on Ω (uniformly with respect to n), i.e.

$$\rho^{(n)}(\mathbf{x}) \le \rho_{\max} \quad \forall\,\mathbf{x}\in\Omega,\ n\ge 0 \tag{2.8}$$

REMARK 2.4. From a theoretical point of view, this assumption might be a severe restriction applying the present steady–state particle method: obtaining *a priori* bounds on the (local) density is crucial in proving the existence of steady–state solutions. We refer the reader to Ref. [6], where the authors give a global existence result for the one–dimensional slab geometry with diffusive boundary conditions. Here, it is crucial that the collision scattering kernel is truncated at small velocities to obtain *a priori* bounds on the (local) density in terms of the momentum flux. Otherwise, the arguments of the proof given there will not go through. On the other hand, applying a standard time–dependent particle scheme for the (multi–dimensional) Boltzmann equation implicitly includes the assumption, that the density is locally bounded; this assumption is even necessary for Maxwellian molecules.

Assuming condition (2.8), we may consider the iteration

$$\frac{\varepsilon}{\rho_{\max}}\mathbf{v}\cdot\nabla f^{(n+1)} + f^{(n+1)} = \left(1-\frac{\rho^{(n)}}{\rho_{\max}}\right) f^{(n)} + \frac{1}{\rho_{\max}} Q_+(f^{(n)})$$

which leads to

$$f^{(n+1)} = \langle \mathrm{e}^{-tD}\Psi[f^{(n)}]\rangle, \tag{2.9}$$

where

$$\Psi[f^{(n)}] = \left(1-\frac{\rho^{(n)}}{\rho_{\max}}\right) f^{(n)} + \frac{1}{\rho_{\max}} Q_+(f^{(n)}), \quad D = \frac{\mathbf{v}}{\rho_{\max}}\nabla$$

In contrast to the previous iteration process, the operator D is now again independent of $\mathbf{x}$ and n, such that $\mathrm{e}^{-tD}\Psi$ is the solution of the free flow equation

$$\frac{\partial f}{\partial t} + \frac{\mathbf{v}}{\rho_{\max}}\nabla f = 0$$

with initial condition Ψ. Moreover, the resulting characteristic system reads

$$\dot{\mathbf{x}} = \frac{\mathbf{v}}{\rho_{\max}} \quad \dot{\mathbf{v}} = 0 \tag{2.10}$$

which yields a system of equations for the particle trajectories in the free flow step, which is as simple as in the one–dimensional case.

It remains to study in more detail the operator $\Psi[f]$: a straightforward observation is, that the operator Ψ conserve the first five moments of the density f, i.e. we have

$$\int_{\boldsymbol{R}^3} \begin{pmatrix} 1 \\ \mathbf{v} \\ |\mathbf{v}|^2 \end{pmatrix} \Psi[f](\mathbf{v})\mathrm{d}\mathbf{v} = \int_{\boldsymbol{R}^3} \begin{pmatrix} 1 \\ \mathbf{v} \\ |\mathbf{v}|^2 \end{pmatrix} f(\mathbf{v})\mathrm{d}\mathbf{v}$$

Moreover, passing to the weak form of $\Psi[f]$, the operator may be identified as an explicit time–discretization of a spatial homogeneous Boltzmann equation with initial condition $f(\mathbf{v})$: first, we consider the normalized density $\tilde{f} = \frac{1}{\rho} f$ together with the corresponding equation for $\tilde{f}$. With the notation $\rho\tilde{\Psi}[\tilde{f}] = \Psi[\tilde{f}]$ the transformed operator reads

$$\tilde{\Psi}[\tilde{f}] = \left(1-\frac{\rho^{(n)}}{\rho_{\max}}\right)\tilde{f} + \frac{\rho^{(n)}}{\rho_{\max}} Q_+(\tilde{f}) \tag{2.11}$$

and $\int \tilde{f} d\mathbf{v} = 1$ for all $\mathbf{x} \in \Omega$.
The (normalized) density function $\tilde{f}(\mathbf{x}, \mathbf{v})$ is for $\mathbf{x} \in \Omega$ fixed the density of a probability measure on $I\!R^3$ with respect to $\mathbf{v}$. Then, $\tilde{\Psi}[\tilde{f}]$ is identified as the solution of an explicit time discretization of the space–uniform Boltzmann equation, where the positivity of $\tilde{\Psi}[\tilde{f}]$ is guaranteed by (2.8).

REMARK 2.5. In particular, because $\tilde{f}$ is normalized to one, we can write

$$\int_{I\!R^3} \Phi(\mathbf{v}) \tilde{\Psi}[\tilde{f}](\mathbf{v}) d\mathbf{v} = \int_{I\!R^3} \Phi(\mathbf{v}) \left(\frac{\rho^{(n)}}{\rho_{\max}} Q_+(\tilde{f}) + \left(1 - \frac{\rho^{(n)}}{\rho_{\max}}\right) \tilde{f} \right) d\mathbf{v}$$

$$= \int_{I\!R^3 \times I\!R^3 \times S^2} \left(\frac{\rho^{(n)}}{\rho_{\max}} \Phi(\mathbf{v}') + \left(1 - \frac{\rho^{(n)}}{\rho_{\max}}\right) \Phi(\mathbf{v}) \right) \cdot$$

$$g(\mathbf{n}) \tilde{f}(\mathbf{v}) \tilde{f}(\mathbf{v}_*) d\omega(\mathbf{n}) d\mathbf{v}_* d\mathbf{v}$$

Hence, if we denote by $\mu_{\tilde{\Psi}}$ and μ the measures with densities $\tilde{\Psi}[\tilde{f}](\mathbf{v})$ and $\tilde{f}(\mathbf{v})$, respectively, the corresponding measure formulation for $\tilde{\Psi}[\tilde{f}]$ reads

$$\mu_{\tilde{\Psi}} = (\mu \times \mu \times \omega \times \lambda) \circ T^{-1} \tag{2.12}$$

where λ denotes the uniform measure on $[0, 1]$ and the transformation T is given by

$$T(\mathbf{v}, \mathbf{v}_*, n, s) = \begin{cases} \mathbf{v}' & \text{if } s \leq \rho^{(n)}/\rho_{\max} \\ \mathbf{v} & \text{else} \end{cases}$$

Because the multi–dimensional steady–state scheme is a generalization of the one used in the one–dimensional case, we describe in the following only the differences in the corresponding particle algorithms: Both schemes use a generalized splitting method to separate the free flow from binary collisions.

1. in both schemes each particle $(\mathbf{x}_i, \mathbf{v}_i)$ is equipped with an individual Poisson–distributed time step t_i. The particle trajectory in the one–dimensional case is given by $x_i(t_i) = x_i + t_i v_i$; whereas in the multi–dimensional case the particle moves with the modified velocity $\mathbf{v}_i/\rho_{\max}$.

2. in the collision stage, each particle undergoes a collision in the one–dimensional case; whereas in multi–dimension there is a collision probability $\rho^{(n)}/\rho_{\max}$ for a collision. In particular, the collision probability if independent of the particle velocities and only depends on the local density $\rho^{(n)}(\mathbf{x})$.

In order to determine the collision probability $\rho^{(n)}/\rho_{\max}$ in the collision stage, one has to evaluate the density at the n–th iteration step using the given particle ensemble for the density $f^{(n)}$. This part is obviously related with the collision process itself and the smoothing kernel $\beta^{\Delta}(\mathbf{x}, \mathbf{x}_*)$ applied to perform the collisions is used to compute $\rho^{(n)}$.

In particular, using the standard smoothing kernel based on a partition of Ω into a cell system, the parameter $\rho_{\max}$ has to be specified as the maximal particle number per cell occurring during the simulation. Then, the collision probability is simply given as the ratio of the present particle number at the n–th iteration and the maximal value $\rho_{\max}$.

Because the collision process is based on some stochastic elements, one may expect that the fluctuations on the particle numbers are less severe than using the direct

analogon of the one—dimensional steady–state scheme discussed in the previous section. One may validate this conjecture by numerical experiments: in Section 3, we give some results on the numerical simulation using steady–state schemes. In particular, we compute the numerical solution of the one–dimensional heat transfer problem, which was already investigated by Bobylev and the author in Ref. [5]; but using the steady–state scheme described above, i.e. we perform a simulation without using the mass coordinate.

2.2. The Treatment of Non–Maxwellian Molecules. With the same idea like in the previous section, i.e. to assume a bounded collision frequency in each iteration step (as defined by assumption (2.8)), one may derive a particle scheme for the full multi–dimensional Boltzmann equation with arbitrary scattering kernels. Besides assumption (2.8), we further have to assume that the given collision scattering kernel is truncated to obtain a bounded collision frequency.
Here, we consider the steady–state Boltzmann equation given by

$$\mathbf{v} \cdot \nabla f + \frac{\nu[f](\mathbf{x})}{\varepsilon} f = \frac{1}{\varepsilon} Q_+(f)$$

with collision operator

$$Q_+(f) = \int_{\mathbb{R}^3} \int_{S^2} g\left(|\mathbf{v} - \mathbf{v}_*|, \frac{(\mathbf{v} - \mathbf{v}_*, \mathbf{n})}{|\mathbf{v} - \mathbf{v}_*|}\right) f(\mathbf{v}') f(\mathbf{v}'_*) \mathbf{d}\mathbf{n}\mathbf{d}\mathbf{v}_*$$

and

$$\nu[f](\mathbf{x}) = \int_{\mathbb{R}^3} \int_{S^2} g f(\mathbf{v}_*) \mathbf{d}\mathbf{n}\mathbf{d}\mathbf{v}_*$$

Like in the previous section, the straightforward iteration reads

$$f^{(n+1)}(\mathbf{x}, \mathbf{v}) = (1 + \frac{\varepsilon}{\nu[f^{(n)}]} \mathbf{v}\nabla)^{-1} \frac{1}{\nu[f^{(n)}]} Q_+(f^{(n)}) \tag{2.13}$$

but applying the iterative process (2.13) is even more complicated than in the previous one using Maxwellian molecules. Here, the collision frequency is even a $\mathbf{v}$–dependent function, which in general is unbounded on $\mathbb{R}^3$. The corresponding characteristic system for the free transport equation

$$\frac{\partial g}{\partial t} + \frac{\mathbf{v}}{\nu[f^{(n)}]} \nabla g = 0$$

which is obtained applying the operator identity (2.4) now reads

$$\dot{\mathbf{x}} = \frac{1}{\nu[f^{(n)}](\mathbf{x}, \mathbf{v})} \mathbf{v} \quad \dot{\mathbf{v}} = 0$$

In order to determine the particle trajectories using a particle method even means to evaluate the collision frequency $\nu[f^{(n)}](\mathbf{x}, \mathbf{v}_i)$ for a given particle velocity $\mathbf{v}_i$. It is obvious, that this kind of approach will lead to a computational effort much higher than applying a standard time–dependent particle method. The resulting particle code will have a computational effort of order n_{loc}^2, where n_{loc} denotes, e.g., the local

particle number per cell, whereas in standard scheme the effort is linear in n_{loc}. Hence, the iteration (2.13) is substituted by

$$\frac{\varepsilon}{\nu_{\max}}\mathbf{v}\nabla f^{(n+1)} + f^{(n+1)} = \left(1 - \frac{\nu[f^{(n)}]}{\nu_{\max}}\right) f^{(n)} + \frac{1}{\nu_{\max}} Q_+(f^{(n)}) \tag{2.14}$$

which is obtained from the assumption that the collision frequencies $\nu[f^{(n)}]$ are uniformly bounded by $\nu_{\max}$, i.e.

$$\nu[f^{(n)}](\mathbf{x}, \mathbf{v}) \leq \nu_{\max} \quad \forall \mathbf{v} \in I\!R^3,\ \mathbf{x} \in \Omega,\ n \geq 0 \tag{2.15}$$

REMARK 2.6. Condition (2.15) implicitly includes the assumption, that the densities $\rho^{(n)}$ are uniformly bounded, because the collision frequency is homogeneous in the density. Furthermore, we have to substitute the scattering kernel g in the collision integral by a truncated kernel $\tilde{g}$. This kind of cut–off is general used in numerical methods for the Boltzmann equation and even necessary in the case of time–dependent scheme, when using non–Maxwellian molecules.

Following the same lines as in the previous section, we can write Eq. (2.14) in the more compact form

$$f^{(n+1)} = \langle \mathrm{e}^{-tD} \Psi[f^{(n)}] \rangle \tag{2.16}$$

where $\Psi[f^{(n)}]$ is now given by the formula

$$\Psi[f^{(n)}] = \left(1 - \frac{\nu[f^{(n)}]}{\nu_{\max}}\right) f^{(n)} + \frac{1}{\nu_{\max}} Q_+(f^{(n)}) \tag{2.17}$$

and the operator D is given by $D = \mathbf{v}\nabla/\nu_{\max}$.

Moreover, one notices, that the collision term given in Eq. (2.17) is quite similar to the corresponding expression for Maxwellian molecules. Like in the previous section, the collision term Ψ conserves the first five moments of the density function and describes an explicit time discretization of the space–homogeneous Boltzmann equation. Again, we have to be a little bit careful, because here we cannot assume, that the densities $f^{(n)}$ are normalized to one, i.e. to perform the collisions, we have to consider the normalized densities, like discussed in the previous section: we denote by $\tilde{f}$ the normalized density of f in the form $\tilde{f} = f/\rho$, where $\rho = \int f(\mathbf{x}, \mathbf{v})\mathrm{d}\mathbf{v} \neq 1$ and write $\rho\tilde{\Psi}[\tilde{f}] = \Psi[\tilde{f}]$. Then, the transformed collision operator reads

$$\tilde{\Psi}[\tilde{f}^{(n)}] = \left(1 - \frac{\rho^{(n)}\nu[\tilde{f}^{(n)}]}{\nu_{\max}}\right) \tilde{f}^{(n)} + \frac{\rho^{(n)}}{\nu_{\max}} Q_+(\tilde{f}^{(n)}) \tag{2.18}$$

and referring to the previous section, Eq. (2.18) is an explicit discretization for the normalized density $f^{(n)}$ with artificial time step $\rho^{(n)}/\nu_{\max}$.

Hence, the steady–state particle method for non–Maxwellian molecules in the multi–dimensional case may again be seen as a generalized splitting method: to derive a simulation algorithm one applies the iteration process (2.16) together with an appropriate beginning condition $f^{(0)}$. In particular, the density $f^{(n+1)}$ is derived from the previous iteration by two fractional steps, which may be denoted as a generalized splitting method.

1. In a first step, one computes a particle approximation for the (modified) collision operator $\Psi[f^{(n)}]$ defined be (2.17). This is done by performing an explicit time

discretization for the space–homogeneous Boltzmann equation with initial condition $\tilde{f}^{(n)} = f^{(n)}/\rho^{(n)}$, i.e. the normalized density of the n–th iteration $f^{(n)}$. In particular, the collision probability of two colliding particles is given by $\rho^{(n)}/\nu_{\max}$, which corresponds to an artificial time step $\rho^{(n)}/\nu_{\max}$ (for the normalized density $\tilde{f}^{(n)}$).

2. The resulting particle approximation for $\Psi[f^{(n)}]$ is used in a second step to apply a time averaging on the operator $e^{-tD}\Psi[f^{(n)}]$ over a Poisson distribution with mean value $\langle t \rangle = \varepsilon$. Here, each particle is equipped with an individual time step (Poisson–distributed) and this time step is used to compute the particle trajectory according to the characteristic system

$$\dot{\mathbf{x}} = \frac{\mathbf{v}}{\nu_{\max}}, \quad \dot{\mathbf{v}} = 0$$

The boundary conditions for the steady–state problem are incorporated in the same way as for time–dependent schemes: if the particle trajectory crosses the boundary of the computational domain, one modifies the trajectory according to the given boundary condition.

3. Numerical Examples.

3.1. One–Dimensional Heat Transfer Problem. As first example for steady flow simulations, we compute the solution for the one–dimensional heat transfer problem between two parallel plates with diffusive boundary conditions, which was already investigated in by Bobylev and the author in Ref. [5]. Here, we use, in contrast to the previous results, the particle method for the multi–dimensional Boltzmann equation as derived in Section 2.1; in particular, we consider the original slab geometry and do not pass to the mass coordinate along the slab.

We compare a standard time–dependent simulation based on the splitting method with the iterative particle scheme derived from the steady–state Boltzmann equation. In particular, the iterative scheme for the steady–state equation is based on the assumption, that the densities $\rho^{(n)}$ at each iteration step are uniformly bounded by $\rho_{\max}$ and the parameter $\rho_{\max}$ is included in the simulation procedure within the free flow of particles and the collision stage: in the free flow step, the velocity of each particle is modified by the factor $1/\rho_{\max}$; in the collision step the probability of a binary collision is equal to $\rho^{(n)}/\rho_{\max}$.

The Knudsen number is varied in a range from 0.02 to 2, where in each simulation the number of spatial cells is fixed at $M = 128$. Moreover, the initial condition is chosen to be a global Maxwellian distribution with (normalized) density and temperature equal to 1 and 200 particles per cell are used to approximate the initial condition, which corresponds to 25.600 particles along the complete slab geometry. The two wall temperatures are kept fixed at $T(0) = 1 \quad T(1) = 2$ and we perform the computations on a nCUBE 2S parallel computer using 32 nodes, such that each processors computes the solution on 4 spatial cells. Finally, the random number generator used in the simulation is the standard *drand48()*–subroutine and on each processor we use a different initialization for the generator. The time step for the time–dependent simulation is given as the inverse of the number of cells, which is obtained from the assumption that the mean velocity of particle is equal to one. The parameter $\rho_{\max}$ for the steady–state scheme was varied from 1.1 for $\varepsilon = 2$ up to 1.6 for $\varepsilon = 0.02$.

REMARK 3.1. The parameter $\rho_{\max}$ is chosen using an *a priori* guess on the maximal density along the slab geometry. Numerical experiments show that the results are nearly independent of $\rho_{\max}$ within a reasonable range of this parameter.

The following two figures (Fig. 1 and 2) show the steady-state density and temperature profiles along the slab geometry. The symbol "A" (solid lines) indicates the solutions obtained from the steady–state simulation, the symbol "B" (dotted lines) the corresponding results using the time–dependent approach. Due to the small time step, which is used in the time–dependent scheme, both methods give nearly identical results at various Knudsen numbers (here, $\varepsilon = 2, 0.5, 0.1$ and 0.02)

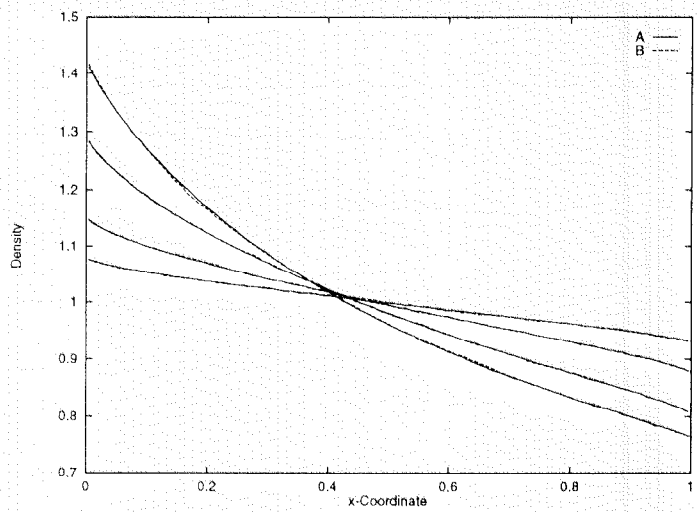

FIG. 1. *Stationary Density Profile*

In both figures, the results for larger Knudsen numbers are identified by the curves with smaller slope.

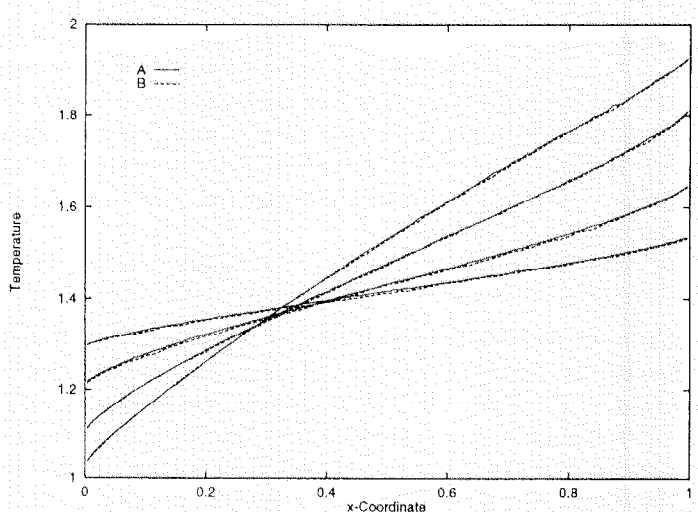

FIG. 2. *Stationary Temperature Profile*

It remains to recover the faster convergence of the steady–state simulation compared with the time–dependent scheme, which was detected in the previous results presented in Ref. [5]. Fig. 3 shows the convergence history of the temperature at the

TABLE 1
CPU times in min:sec.

Scheme	$\varepsilon = 2.0$	$\varepsilon = 0.5$	$\varepsilon = 0.1$	$\varepsilon = 0.02$
A	85:33	65:04	62:32	57:60
B	25:29	26:56	30:42	39:29

right boundary cell, which is obtained as the arithmetic average over the iterations or time steps, respectively.

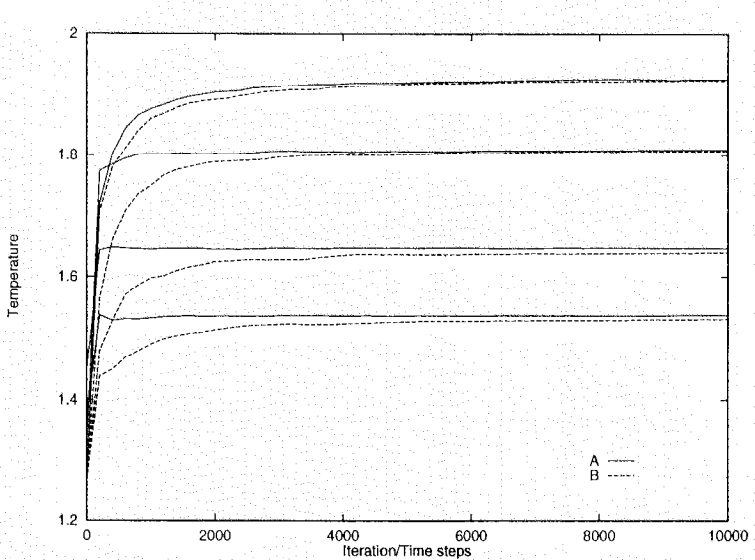

FIG. 3. *Convergence History for the Right Boundary Cell*

Again the steady–state scheme yields a much faster convergence at Knudsen numbers of the order 1; whereas for the smaller Knudsen numbers (here, the smallest Knudsen number is $\varepsilon = 0.02$) the convergence of both schemes is nearly the same.

The CPU times for 20.000 iterations or time steps, respectively, are summarized in Table 1. Due to the larger number of collisions in the steady–state simulation as well as the larger number of gas–surface interactions in the free flow step, the steady–state method is again more time–consuming.

In particular at Knudsen numbers of order 1, this additional effort is compensated by the faster convergence of the steady–state scheme.

3.2. Simulation of Benard's Instability by Steady–State Schemes. Here we are concerned with the natural convection of a gas enclosed between two parallel plates, where the gas is heated from below; which is known as the so–called Benard–convection. This problem is of special interest, because it contains the formation of special flow patterns as well as a transition to turbulence: for moderate temperature differences between the upper and lower wall, the gas remains in a stable equilibrium state with a density increasing vertically upwards. If the temperature is increased over a certain threshold value, which even depends on the distance between the two walls, the gas starts to form a certain number of horizontal vortices. Finally, for larger temperature differences, a transition to turbulence occurs.

REMARK 3.2. To detect a transition to turbulence in a rarefied gas certainly defines on of the most challenging problems in the numerical simulation of rarfied gas

flows. Here, the simulation of Bénards's instability is an appropriate test case, if one considers the fully three–dimensional configuration.

In the following, we consider Benard's instability for a rarefied gas flow in two space dimensions, which was already investigated by Stefanov and Cercignani in Ref. [10] using the (time–dependent) Direct Simulation Monte Carlo (DSMC) method of Bird [2]. We are in particular interested in applying the steady–state particle scheme of Section 2.2, in the cases, where a formation of stable vortices can be observed using a time–dependent scheme (see Ref. [10]).

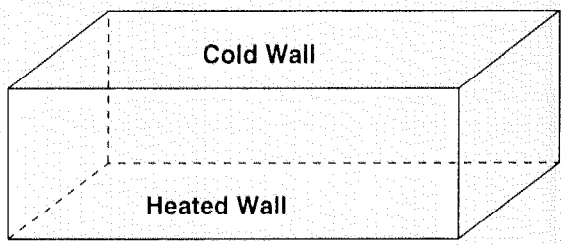

FIG. 4. *Rarefied gas between two parallel plates*

The (time–dependent) problem is described by the standard (two–dimensional) Boltzmann equation; but the equation includes a (gravitational) force $F = (0, g)^t$, $g > 0$, which accelerates each gas particle vertically downwards,

$$f_t + \mathbf{v}\nabla f - g\partial_v f = \frac{1}{\varepsilon} Q(f) \tag{3.1}$$

with spatial coordinate $\mathbf{x} = (x, y) \in \Omega$, velocity $\mathbf{v} = (u, v, w) \in I\!R^3$ and density function $f = f(t, \mathbf{x}, \mathbf{v})$. In the collision operator Q we assume a collision scattering kernel describing the hard–sphere interaction model. For the corresponding initial–boundary value problem on the spatial domain $\Omega = [0, L_x] \times [0, L_y]$, Eq. (3.1) is equipped with an initial condition,

$$f(0, \mathbf{x}, \mathbf{v}) = \overset{o}{f}(\mathbf{x}, \mathbf{v}), \quad \mathbf{x} \in \Omega, \, \mathbf{v} \in I\!R^3$$

and some boundary conditions on $\partial\Omega$: at the two horizontal plates, we assume diffusive reflection according to the wall temperatures T_h and T_c. For the two other walls involved in this problem, we use specular reflecting boundary conditions.

REMARK 3.3. Like stated in the previous work by Stefanov and Cercignani [10], this corresponds to periodic boundary conditions on a larger domain $\bar{\Omega}$ with size $[0, 2L_x] \times [0, L_y]$ and therefore reduces the computational effort performing numerical simulations on $\bar{\Omega}$.

It is well–known, that the standard Boltzmann equation without force term contains two dimensionless parameters, which completely characterize the problem above. This two parameters are the Knudsen number ε, which balances the influence of binary collisions on the free transport of particles as well as the temperature ratio T_c/T_h of the two horizontal walls.

REMARK 3.4. In the case of the corresponding steady–state equation, even the total mass contained in the spatial domain Ω yields a parameter, which characterize a steady–state solution. Here, we refer the reader to the discussion given in Ref. [6].

The situation changes, if the Boltzmann equation contains a force term like in Eq. (3.1): because the particles are accelerated vertically downwards, even the distance

between the two horizontal walls yields a free parameter determining the solution of the problem. In Ref. [10] the authors used the so–called Froude number Fr based on the thermal speed $v_h = (2RT_h)^{1/2}$ to specify this third parameter. Moreover, the authors related the three dimensionless parameters of the rarefied gas flow to the Rayleigh number of the problem applying a continuum fluid model. Rayleigh obtained this non–dimensional parameter by analyzing the stability of solutions using a linearization of the Navier–Stokes system in the Boussinesq approximation [9]. In particular, the Rayleigh number yields the above mentioned threshold value for the transition from a stable equilibrium flow to the formation of stable vortices, we refer the reader to the material given, e.g., in Ref. [8]).

The force term in Eq. (3.1) leads to modified particle trajectories applying a particle scheme to the time–dependent as well as steady–state equation. In the case of time–dependent problems, where one uses the splitting method, the corresponding free transport equation reads

$$\frac{\partial f}{\partial t} + \mathbf{v}\nabla f - g\partial_w f = 0$$

This equation is solved by the characteristic system

$$\dot{\mathbf{x}} = \mathbf{v}, \quad \dot{v} = 0, \quad \dot{w} = -g, \quad \dot{z} = 0$$

and the particle trajectories over the (fixed) discrete time step Δt of a particle located at the position $\mathbf{x}_i = (x^{(i)}, y^{(i)})$ with velocity $\mathbf{v}_i = (v^{(i)}, w^{(i)}, z^{(i)})$ is given by

$$\left\{ \begin{array}{ll} x^{(i)}(\Delta t) = x^{(i)} + \Delta t v^{(i)} & v^{(i)}(\Delta t) = v^{(i)} \\ y^{(i)}(\Delta t) = y^{(i)} + \Delta t w^{(i)} - (\Delta t)^2 g/2 & w^{(i)}(\Delta t) = w^{(i)} - \Delta t g \\ z^{(i)}(\Delta t) = z^{(i)} & \end{array} \right. \tag{3.2}$$

Hence, the particle trajectories are no longer straight lines, but parabolic curves in the y–component of the particle trajectory; additionally, the particle velocity w does not remain constant along the free transport. In particular, one has to change the treatment of boundary conditions, when the particle trajectory intersects one of the two horizontal walls, where diffusive boundary conditions are prescribed.

REMARK 3.5. For the other two walls involved in the problem, we assumed specular reflecting boundary conditions and the treatment of this kind of boundary conditions does not change including the force term, because the force acts parallel to the boundaries.

For particle trajectories, which intersect with the horizontal walls, one has to determine the exact intersection point as well as the remaining time step, with which the particle will move with new velocity when applying diffusive boundary conditions. In particular, this means to solve a quadratic equations for the discrete time step, which obviously yields an appropriate parameterization of the trajectory.

Besides the fact, that one needs to determine the "correct" root of the quadratic equation to compute the exact intersection point, the quadratic equation itself is even – in general – singular perturbed. Introducing dimensionless quantities, one finds that the parameter describing the gravitational force is a small parameter, i.e. $g \ll 1$. Moreover, this parameter appears in front of the quadratic term of the equation, from which one can conclude, that one root of the quadratic equation tends to $\pm\infty$ as g tends to zero.

REMARK 3.6. In particular this means, that the particle trajectories degenerate in the limit $g \to 0$ again to straight lines.

Hence, to reduce the computational effort determining the exact intersection point of a given particle trajectory with the horizontal walls, it is reasonable to consider an asymptotic expansion for the correct root of the quadratic equation. This is demonstrated in the following example.

EXAMPLE 3.7. Let us assume, that a particle is located at $y_0 > 0$ on the y–axis and moves with velocity $w_0 < 0$ in a weak force field according to the trajectory

$$y(t) = y_0 + w_0 t - \varepsilon \frac{t^2}{2}$$

where $\varepsilon \ll 1$ describes the force field. Moreover, we assume, that there exists a time T, such that $y(T) < 0$, i.e. the particle crosses the origin of the y–axis at some time t_c and we want to compute this crossing time. Then, we have to solve the quadratic equation

$$\varepsilon \frac{t^2}{2} - w_0 t = y_0, \tag{3.3}$$

which yields the two roots

$$t^{\varepsilon}_{\pm} = \frac{1}{\varepsilon}\left(w_0 \pm (w_0^2 + 2\varepsilon y_0)^{1/2}\right) \tag{3.4}$$

In particular, if $\varepsilon = 0$, the single root reads $t^{(0)} = -y_0/w_0$ and on of the solutions given in (3.4) runs to $\pm\infty$ in the limit $g \to 0$. Assuming $\varepsilon \ll 1$, one may compute the correct crossing time t^{ε}_c using an asymptotic expansion of t^{ε}_c as follows: we assume that t^{ε}_c has an asymptotic expansion of the form

$$t^{\varepsilon}_c \sim \sum_{i=0}^{k} \varepsilon^i t_i \tag{3.5}$$

REMARK 3.8. Concerning the notion "asymptotic expansion" we refer the reader to the textbook of Bleistein and Handelsmann given in Ref. [3]

Substituting (3.5) into Eq. (3.3) and comparing powers in ε leads to a system of equations for $\{t_0, \ldots, t_k\}$ and for the first two coefficients one obtains the relations

$$t_0 = -y_0/w_0 \quad t_1 = y_0^2/(2w_0^3)$$

Hence, the first order expansion for t^{ε}_c is given in the form

$$t^{\varepsilon}_c \sim -\frac{y_0}{w_0} + \varepsilon \frac{y_0^2}{2w_0^3}$$

It is trivial to notice, that the zeroth order expansion exactly yields the single solution $t^{(0)}$ in the limit $\varepsilon \to 0$.

The simulation codes applied in the following use – in general – the first order expansion for the intersection times of particle trajectories, which cross the two horizontal planes. Here, in general means, that the first order expansion fails, if the first order correction $\varepsilon t^{(1)}$ itself is of order $O(1)$, e.g., if $w_0 = O(\varepsilon)$ and $w_0 = O(\varepsilon)$.

For the steady–state schemes of Section 2.2, one includes the force term in the simulations as follows: the steady–state equation reads

$$\mathbf{v}\nabla f - g\partial_v f = \frac{1}{\varepsilon} Q(f) \tag{3.6}$$

with the same notations as given above. Based on the assumption, that the (local) collision frequencies $\nu[f^{(n)}]$ are uniformly bounded by $\nu_{\max}$, one obtains the iteration process

$$\frac{\varepsilon}{\nu_{\max}}\mathbf{v}\nabla f^{(n+1)} - \frac{\varepsilon}{\nu_{\max}}g\partial_v f^{(n+1)} + f^{(n+1)} = \left(1 - \frac{\nu[f^{(n)}]}{\nu_{\max}}\right) f^{(n)} + \frac{1}{\nu_{\max}}Q_+(f^{(n)}) \tag{3.7}$$

Hence, Eq. (3.7) leads to the iteration

$$f^{(n+1)} = \langle \mathrm{e}^{-tD}\Psi[f^{(n)}]\rangle$$

which is exactly the same as in Section 2.2, except that the operator D is now given by

$$D = \frac{\mathbf{v}}{\nu_{\max}}\nabla - \frac{g}{\nu_{\max}}\partial_v \tag{3.8}$$

Together with Eq. (3.8), the term $\mathrm{e}^{-tD}\Psi[f^{(n)}]$ solves the free transport equation with force term, i.e.

$$f_t + \frac{1}{\nu_{\max}}\left(\mathbf{v}\nabla f - g\partial_v f\right) = 0$$

and initial condition given by $\Psi[f^{(n)}]$. The corresponding characteristic system reads

$$\dot{\mathbf{x}} = \frac{\mathbf{v}}{\nu_{\max}}, \quad \dot{u} = 0,\ \dot{v} = \frac{g}{\nu_{\max}},\ \dot{w} = 0 \tag{3.9}$$

which defines the particle trajectories exactly in the form given in Eq. (3.2) together with a Poisson–distributed time step with mean value ε. Hence, to include the force term in the steady–state equation, one uses the same approach as in the time–dependent scheme, i.e. for each particle one generates a Poison–distributed discrete time steps with mean value equal to ε and solves the characteristic system given in Eq. (3.9) over this time step. The resulting particle trajectories are no longer straight lines, but curved lines and the particles are accelerated vertically downwards. As in the time–dependent scheme, one may use the asymptotic expansion method given above to reduce the computational effort necessary to compute the particle interaction with solid walls.

In the following, we give numerical results on a rarefied gas flow close to the continuum limit, where one may expect the formation of vortices. In the previous work by Stefanov and Cercignani [10], the formation of vortices was observed at a Knudsen number of 0.01 together with a temperature ratio $r = 0.1$ and a modified Froude number of $Fr^* = Fr/Kn = 200$. Here, using a similar range for the temperature ratio r and the modified Froude number Fr^*, we show that Benard's instability may even be detected at larger Knudsen numbers, e.g. $Kn = 0.02$.

The two–dimensional computational domain is fixed at a size of $[300, 100]$, such that a Knudsen number of 0.02 yields a mean free path of 2. This domain in divided into 192×64 cells, which gives a total number of cells equal to 12.288. Moreover, we use approximately 10 particles per cell, i.e. a total number of about $1.2 \cdot 10^5$ particles to approximate the solution on the complete phase space. As initial condition for the time–dependent simulation as well as beginning condition for the steady–state

iteration we use a global Maxwellian distribution with (normalized) density $\rho_\infty = 1$ and temperature $T_\infty = 1$. The upper wall temperature is fixed at $T_c = 0.1$, such that the temperature ratio $r = 0.1$ yields $T_h = 1 = T_\infty$.

REMARK 3.9. In the time–dependent simulation we use a (scaled) time step $\Delta t = 100/64$ for the splitting method, which is obtained from the assumption that the averaged velocity of a particle is equal to one. Moreover, we use 6 local collision cycles to solve the space–homogeneous Boltzmann equation using an explicit time integration scheme. Applying the steady–state simulation, the time step of each particle is Poisson–distributed with mean value equal to the mean free path, i.e. $\langle \Delta t_{\text{steady}} \rangle = 2$ and we take $\nu_{\max} = 4$ as uniformly bound on the collision frequency.

We first give numerical results on the transient formation of vortices applying a time–dependent particle method: starting with a global Maxwellian distribution, we apply a time–integration of the Boltzmann equation over 40.000 discrete time steps. Moreover, at certain stages of the simulation, we perform a local time average to obtain some transient results on the flow field structure. Fig. 5 gives a sequence of transient velocity fields obtained by a local time averaging.

As shown in the sequence of velocity fields, the formation of vortices starts at the first local time average over the time steps 1000-2000. Later on, it seems, that there exist 4 intermediate vortices, where the last small one disappears in the local average from 16.000–20.000 time steps. The flow pattern shown there remains stable up to the end of the simulation (see also Fig. 3.7).

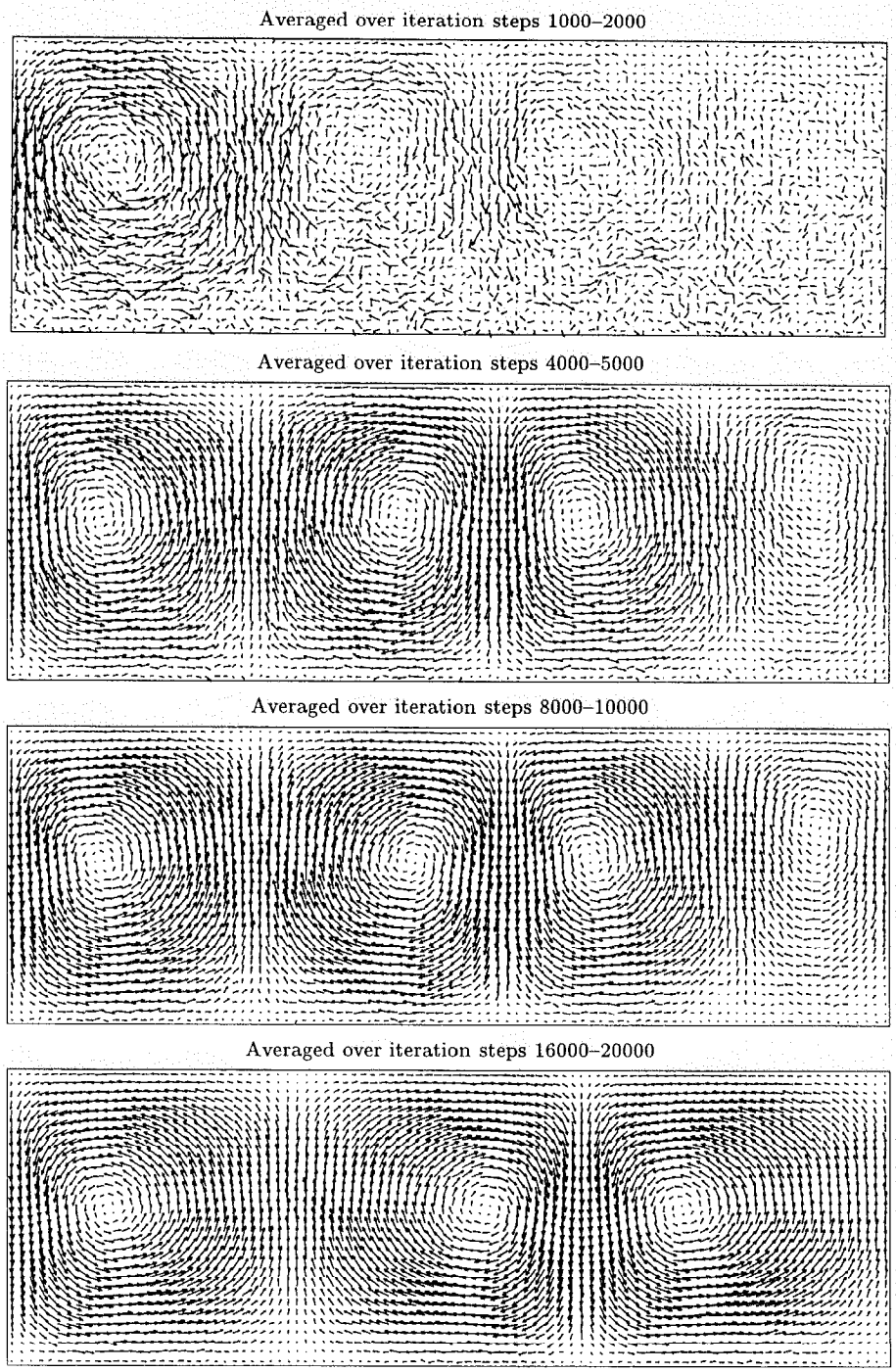

FIG. 5. *Transient Velocity Fields*

The total CPU–time using 64 nodes of a nCUBE 2S parallel computer was about 12 hours for 40.000 discrete time steps. Here, the parallelized code uses a domain decomposition along the x–axis of the computational domain: each processor computes the local solution on a domain of 3×64 cells. After the free flow step of the splitting method, the processors exchange particles, which leave or enter the present processor domain. Because the differences in the local particle number of each processor, this static partition is kept fixed during the simulation.

In a second simulation, we apply the steady–state particle scheme of the previous secion to the corresponding steady–state problem defined by Eq. (3.6). In particular, because the collision scattering kernel describes the hard–sphere interaction model, we use the particle method as discussed in Section 2.2 together with the modifications to include the force term as given above. For the beginning condition $f^{(0)}$ we use the initial condition of the time–dependent problem.

REMARK 3.10. Due to mass conservation along the complete boundary, the steady–state problem contains an additional free parameter, namely the total mass on the spatial domain. Using the initial condition of the time–dependent problem as beginning condition ensures, that the two simulations (time–dependent or steady–state) describe the same problem.

As mentioned above, the individual (artificial) time step of each particle in the iteration is Poisson–distributed with mean value $\langle \Delta t_{\text{steady}} \rangle = 2$. Moreover, we have to choose *a priori* an appropriate bound for the collision frequency. Here, we use $\nu_{\max} = 4$, which is later on, i.e. during the numerical simulation, validated as a reasonable bound.

To compare the results obtained from the steady–state simulation with the previous time–dependent particle method, we give in the following figures the same sequence of local averages; but now averaged over the iteration process: Fig. 6 shows the sequence of transient velocity fields. The results indicate, that although the formation of vortices starts later than in the time–dependent scheme, the formation of the final flow pattern is already achieved after 10.000 iterations. Again, this pattern remains constant up to the end of the simulation defined by 40.000 iterations.

REMARK 3.11. That the formation of vortices starts later than in the time–dependent scheme might be explained by the fact, that the bound $\nu_{\max}$ slows down the particles by the factor $1/\nu_{\max}$ (see the characteristic system given in Eq. (3.9)): together with the mean free path, one has $\langle \Delta t_{\text{steady}} \rangle / \nu_{\max} = 1/2$ compared to $\Delta t = 100/64$ of the time–dependent scheme. One may even notice, that the results obtained from the steady–state method contain slightly higher fluctuations than the corresponding time–dependent scheme. This might arise from the fact, that the steady–state particle scheme contains a further random variate, namely the Poisson–distributed individual time step of each particle applying the generalized splitting method.

The total CPU–time for the steady–state simulation using 40.000 iterations was about 9 hours, again using 64 nodes of a nCUBE 2S parallel machine. Here, the parallelization uses the same domain decomposition approach as the time–dependent one.

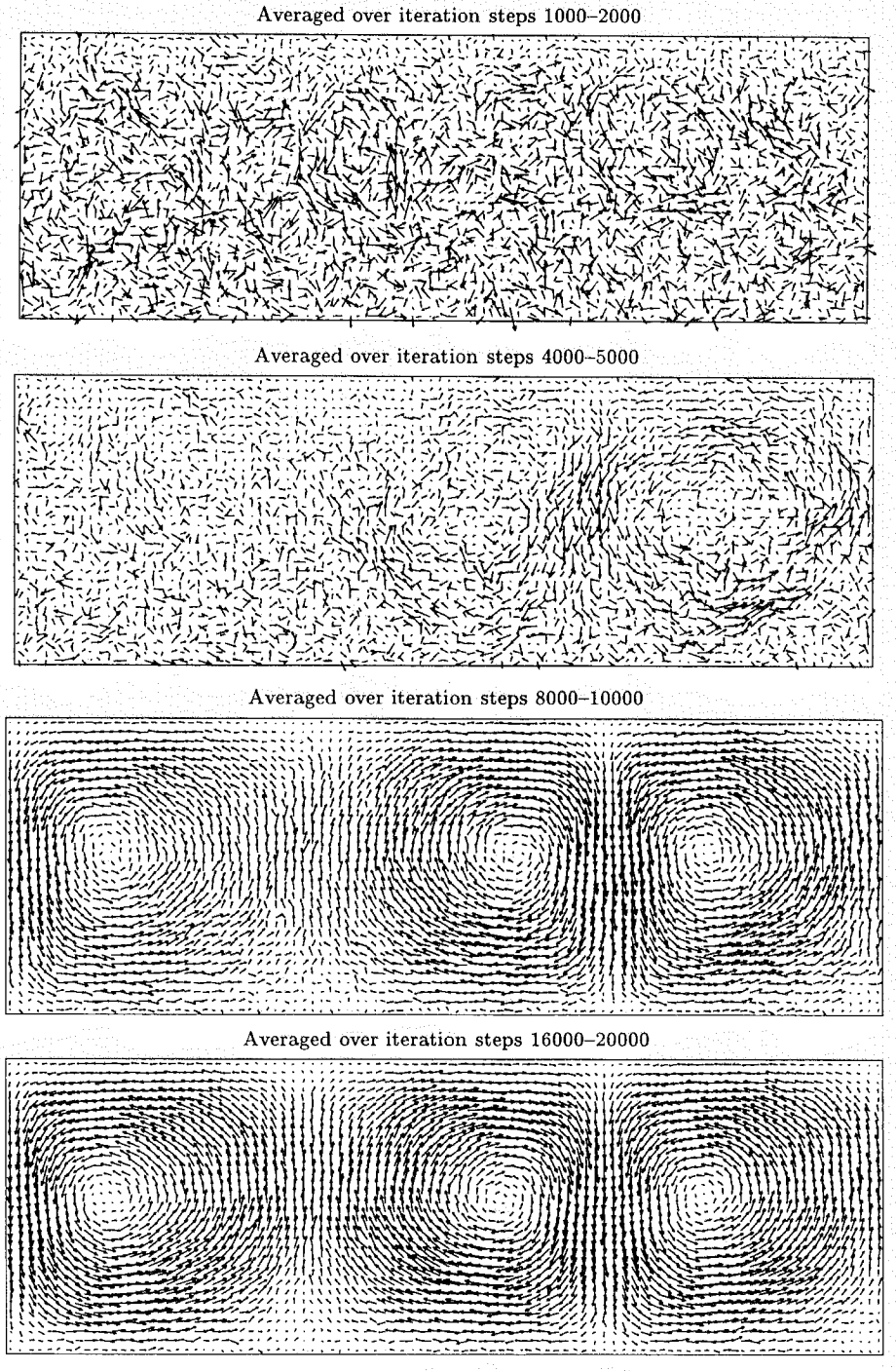

FIG. 6. *Iterated Velocity Fields*

Finally, we compare in Fig. 7 the velocity fields of the two schemes at the end of the simulations, i.e. the local averages over the time steps (or iterations) 36.000–40.000.

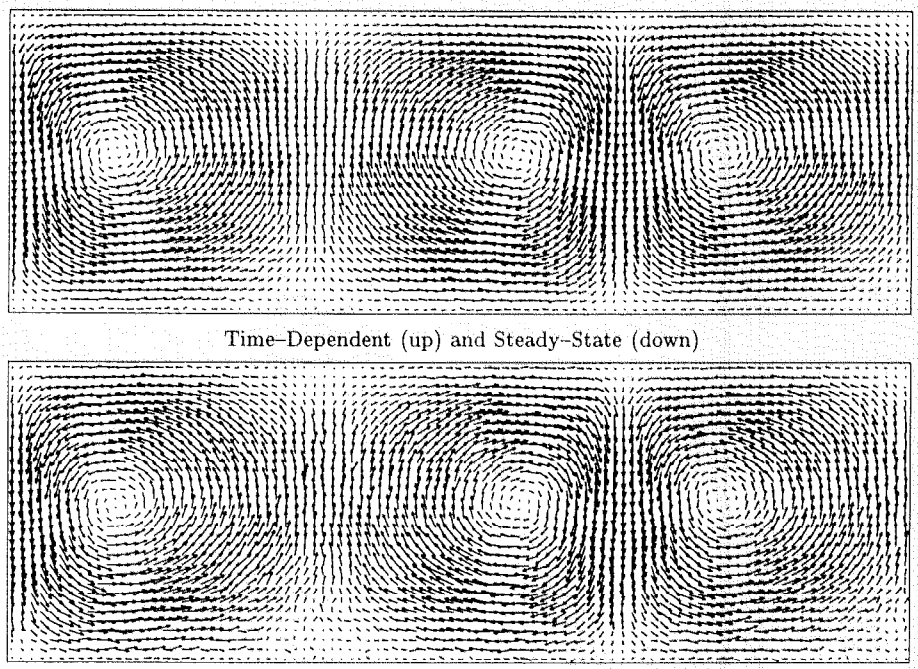

Time–Dependent (up) and Steady–State (down)

FIG. 7. *Final Velocity Fields*

One notices, that both schemes give nearly identical results, where again the steady–state scheme seems to contain more fluctuations (see the remark given above). Some one–dimensional density and temperature profiles along fixed coordinate lines are given in Fig. 8 and 9. Here, one observes a small shift in the density and temperature profiles along the horizontal line at $y \approx 50$; on the other hand the results obtained from the two schemes nearly coincide along the vertical line at $x \approx 200$.

It is not the aim of the current investigation to study in more detail Benard's instability in a rarefied gas flow; although this problem turns out to be the starting point to investigate the transition to turbulence in a rarefied gas: one should perform further simulations using different values for the Knudsen number, the temperature ratio as well as for the Froude number to derive an analogous threshold value (probably depending on the Knudsen number) like the Rayleigh number in continuum flows. Moreover, one should perform fully three–dimensional simulations in order to detect some turbulence phenomena. These topics will be discussed in a subsequent paper.

On the contrary, the numerical simulations given here should demonstrate, that the preliminary results on steady–state schemes given in Ref. [5] are not restricted to the simple one–dimensional case for Maxwellian molecules; but steady–state scheme might even be applied efficiently for multi–dimensional problems together with general collision scattering kernels.

In addition to this, we performed simulations of a rarefied gas flow close to the continuum limit: the previous results on steady–state schemes in the one–dimensional case showed, that the steady–state scheme yields a faster convergence to the steady–state solution than a corresponding time–dependent problem method in particular if

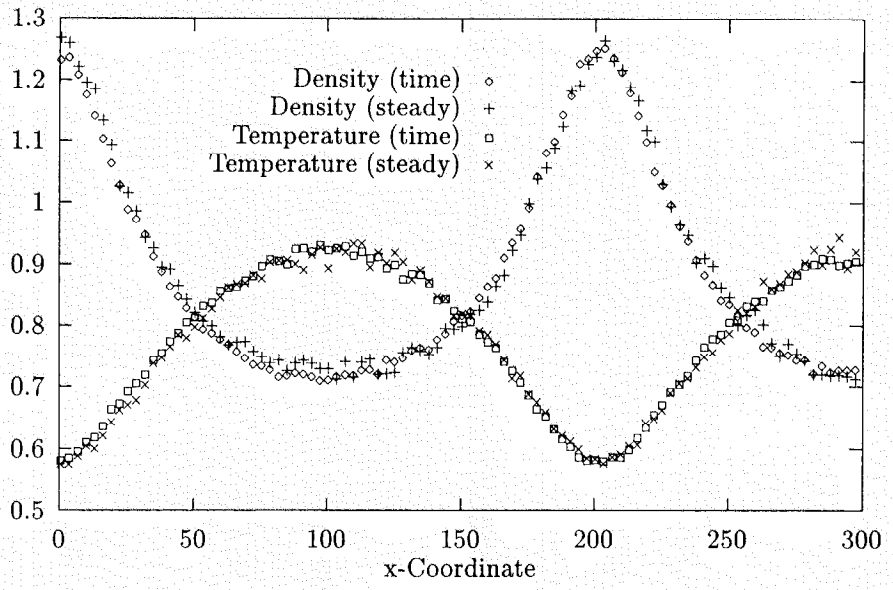

FIG. 8. *Density and Temperature Profiles at fixed* $y \approx 51$

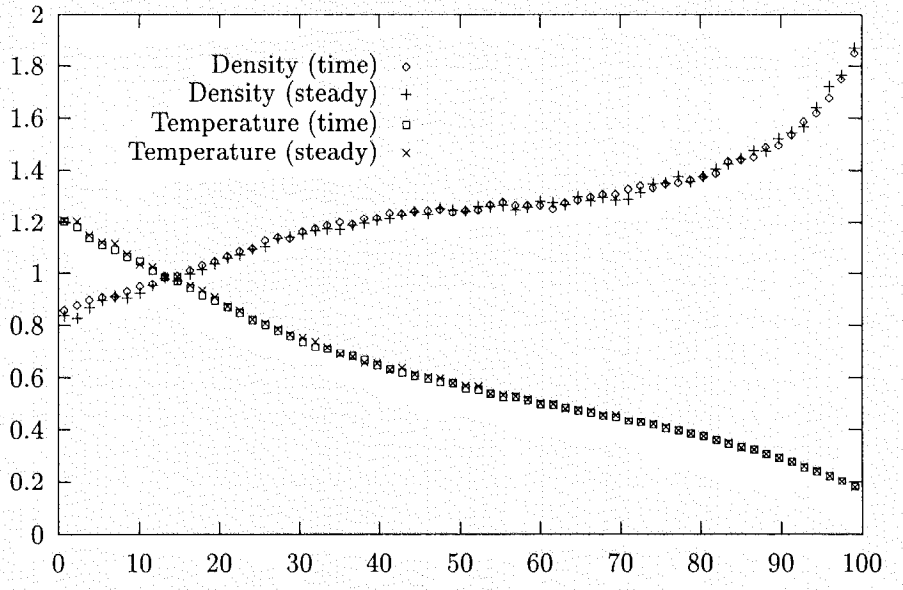

FIG. 9. *Density and Temperature Profiles at fixed* $x \approx 200$

the Knudsen number is of the order 1 and the faster convergence easily compensates the higher computational effort of the steady–state scheme. In the current investigation, the steady–state scheme is even more fast than the corresponding time–dependent scheme: as mentioned above, we used 12 hours CPU–time to compute 40.000 discrete time steps compared to 9 hours for 40.000 iteration steps. Moreover, the results showed, that the iterative process converges about two times faster than the time–dependent method – besides the fact, that we get rid of the time–discretization.

Hence, one might state, that the steady–state scheme yields the more efficient numerical tool than a time–dependent simulation – even close to the continuum limit. This conclusion certainly needs to validated by some further numerical simulations of boundary value problems for the steady–state Boltzmann equation.

4. Conclusion. In the previous sections, we presented some new particle methods, which may be used to simulate boundary value problems of the steady–state Boltzmann equation directly instead of passing to the corresponding time–dependent problem. These schemes may be interpreted as generalized splitting methods, because they are based on a similar approach as time–dependent schemes; namely one uses fractional steps to separate the collisions among the rarefied gas from the undisturbed free transport along particle trajectories defined by the local particle velocity. On the other hand, the particle trajectories of the steady–state methods depend on a stochastic time step for each particle, which is Poisson–distributed with mean value equal to the Knudsen number of the rarefied gas flow.

The steady–state particle methods are derived using a formal and implicit expression for the steady–state solution of the Boltzmann equation. Here, one applies an iteration process to solve the implicit equation and finally obtains the above mentioned generalized splitting method together with the necessary modifications in the free transport step.

Concerning the theoretical foundation of steady–state methods, there remain some questions, which we either did not discussed up to now or even discussed only briefly. First of all, the central question concerns the convergence property of the iterative process applied to the formal expression of the steady–state solution. This problem is obviously independent of the special numerical realization of the iteration using a particle method. In particular, proving the convergence of the iteration process means to prove the existence of a global solution of boundary value problems for the steady–state Boltzmann equation. Hence, applying a steady–state method like given here implicitly assumes the existence of a steady–state solution as well as the convergence of the iteration process applied to the implicit equation.

The treatment of boundary conditions applying a steady–state particle method is certainly related with the previous question. Here, we proposed to include the boundary conditions in the same way as in time–dependent schemes, i.e. one modifies the particle velocity, if the particle trajectory crosses the boundary of the spatial domain during the free transport step of the (generalized) splitting method. Besides the theoretical questions concerning the treatment of boundary conditions, we in particular did not discussed, how to include inflow boundary conditions for the steady–state scheme, which are generic boundary conditions to simulate hypersonic rarefied gas flows around re–entry configurations.

The final remark concerns the convergence of steady–state schemes itself, i.e. the convergence of the discrete particle approximation. Here, on easily finds, that the convergence is proved using the same techniques as used for time–dependent particle methods, accept that one has to include the stochastic time step in the convergence proofs.

The numerical results turned out to be quite promising: the convergence of the steady–state scheme is – at least for moderate Knudsen numbers – much faster than using a conventional time–dependent method and even for flow problems close to the continuum limit, steady–state schemes are at least as good as the conventional time–dependent particle methods.

REFERENCES

[1] H. BABOVSKY, *Time Averages of Simulation Schemes as Approximations to Stationary Kinetic Equations*, Eur. J. Mech., B/Fluids, 11 (1992), pp. 199–212.

[2] G.A. BIRD *Molecular Gas Dynamics and the Direct Simulation of Gas Flows*, Clarendon Press, Oxford, 1994.

[3] N. BLEISTEIN AND R.A. HANDELSMANN, *Asymptotic Expansions of Integrals*, Holt, Rinehart and Winston, New York, 1975.

[4] A.V. BOBYLEV AND J. STRUCKMEIER, *Implicit and Iterative Methods for the Boltzmann Equation*, TTSP, 25 (1996), pp. 175–195.

[5] A.V. BOBYLEV AND J. STRUCKMEIER, *Numerical Simulation of the Stationary One–Dimensional Boltzmann Equation by Particle Methods*, Eur. J. Mech., B/Fluids, 15 (1996), pp. 103–118.

[6] R. ILLNER AND J. STRUCKMEIER *Boundary Value Problems for the Steady Boltzmann Equation* J. Stat. Phys., 85 (1996), pp. 427–454.

[7] H. NEUNZERT AND J. STRUCKMEIER, *Particle Methods for the Boltzmann Equation*, in ACTA NUMERICA 1995, A. Iserles, ed., Cambridge University Press, Cambridge, 1995, pp. 417–457.

[8] L. PRANDTL, K. OSWATITSCH AND K. WIEGHARDT, *Führer durch die Strömungslehre*, Vieweg, Braunschweig, 1984.

[9] LORD RAYLEIGH, *On convective currents in a horizontal layer of fluid when the higher temperature is on the under side*, Philos. Mag., 32 (1916), pp. 529–546.

[10] S. STEFANOV AND C. CERCIGNANI, *Monte Carlo Simulation of Bénard's Instability in a Rarefied Gas*, Eur. J. Mech., B/Fluids, 11 (1992), pp. 543–554.